

## Part II

# Spectroscopic Methods in Homogeneous Hydrogenation

## 11

# Nuclear Magnetic Resonance Spectroscopy in Homogeneous Hydrogenation Research

*N. Koen de Vries*

### 11.1

#### Introduction

##### 11.1.1

#### Nuclear Magnetic Resonance (NMR)

NMR spectroscopy is a very powerful tool for structural characterization purposes. Following the discovery of the technique, organic chemists were quick to recognize its potential and as soon as commercial instruments came on the market they began to use NMR to elucidate the structures of their synthetic efforts. During the late 1960s and early 1970s, some very important developments took place that made the technique what it is today. The first development was that of the so-called Fourier transform (or FT-NMR) measurement [1]. Until then, the magnetic field was varied, and as it swept through the whole frequency range a recorder noted the moment when a nucleus was on resonance. In the FT-mode, all frequencies are excited at the same time by a short pulse, and the response in time of all the nuclei together is recorded as they relax back to equilibrium. The Fourier transformation converts this time-dependent signal to a frequency-dependent signal, which is the NMR-spectrum. As in all FT-techniques, the major advantage is that one can acquire more than one scan. This improves the signal-to-noise ratio because it increases with the square root of the number of scans. From then on, insensitive nuclei such as  $^{13}\text{C}$ -NMR could also be measured routinely. This nucleus has a much larger chemical shift range and thus allows a better resolution.

The second development that has revolutionized the practice of NMR was the introduction of multidimensional spectroscopy. This was initialized by Jeener [2], who showed that, by introducing a second pulse and varying the time between them, a second “time-axis” could be constructed. A double Fourier transformation yields the familiar two-dimensional spectrum, nowadays known by everyone as the COSY spectrum. Ernst, already involved in the development of FT-NMR, showed that the concept was more generally applicable [3], and paved

the way for the whole variety (hundreds, if not thousands) of multidimensional experiments that exist today. A typical and well-known example of what can be achieved is the complete three-dimensional structure elucidation of peptides consisting of hundreds of amino acids.

NMR continued to develop during the 1980s and 1990s with techniques such as inverse NMR [4] and gradient pulses [5]. It would also be valuable to mention here the various instrumental improvements such as cryo-probes and the ever-increasing magnetic-field strength (with commercial 1000-MHz spectrometers almost in reach), all aimed at improving resolution and sensitivity.

It is this relative insensitivity that is usually considered as the major drawback of NMR spectroscopy. However, the flexibility of the NMR technique, with the ability to obtain structural information, quantitative data (e.g. kinetic parameters), as well as an indication of molecular volume, using pulsed gradient spin echo (PGSE) NMR diffusion methods [6], makes NMR a most valuable tool.

### 11.1.2

#### **NMR in Homogeneous Hydrogenation Research**

On the subject of NMR spectroscopy in homogeneous hydrogenation research, we can recognize that most developments have found their way into this research area, albeit with some delay. For example, the PGSE methods had been used for over twenty years to determine diffusion coefficients of organic molecules before their potential in organometallic chemistry was investigated [7]. Pioneering studies were also conducted by von Philipsborn who, during the early 1980s, was already performing transition metal NMR spectroscopy in order to probe structures of organometallic compounds and their reactivity. For further information, the reader is referred to an excellent review on this topic [8].

In this chapter, we will provide an introduction into the application of NMR in the area of homogeneous hydrogenation research, and suggest further reading for those who wish to obtain more information on the subject. The principles of NMR spectroscopy have been covered thoroughly by Ernst [9], and numerous books and review articles have appeared on all aspects of the application of NMR in homogeneous hydrogenation research. Typical reviews include “NMR and homogeneous catalysis” in general [10], “NMR at elevated gas pressures and its application to homogeneous catalysis” [11], the measurement of transition metals by NMR [12] and, more recently, “ $^{103}\text{Rh}$  NMR spectroscopy and its application to rhodium chemistry” [13].

Other important topics, such as the use of *para*-hydrogen-induced polarization (PHIP) NMR, are discussed in more detail elsewhere in this book. Basically, this approach enhances the NMR signal one thousandfold, thus allowing the detection of intermediates that go unnoticed when using “classical” NMR techniques. PHIP is particularly suited for homogeneous hydrogenation research because a prerequisite of the method is that both former *para*-hydrogen nuclei must be present (and J-coupled) in the molecule of interest.

In summary, NMR in homogeneous hydrogenation research is used for:

- Structure elucidation of various species present in the reaction mixtures; typical tools used for this purpose include chemical shifts, coupling constants, PHIP-NMR, and 2D-NMR.
- Determination of reaction mechanisms by combining the observed intermediates in a catalytic cycle. To do this, it is often necessary to measure under different conditions – that is, variable temperature NMR. The use of high-pressure NMR cells is crucial in order to measure under the real catalytic conditions. The EXSY experiment helps to unravel exchange pathways, both intra- and intermolecular.
- Determination of the reaction kinetics if the reaction is slow enough to record a series of NMR spectra. This can be done with standard 1D-NMR measurements if the concentrations are high enough, and if not, by making use of sensitivity enhancement through *para*-hydrogen. NMR experiments designed for kinetic investigations in combination with PHIP techniques include ROCHESTER (Rates Of Catalytic Hydrogenation Estimated Spectroscopically Through Enhanced Resonances) [14] and DYPAS. An example of the investigation of kinetics of homogeneous hydrogenation reactions using both experiments can be found in [15].

## 11.2 NMR Methods

### 11.2.1 General

In order to perform the various tasks mentioned in Section 11.1.2, it is necessary to use one or several methods to gather information by NMR spectroscopy. Typically, chemical shift and coupling constant information, 2D-NMR measurements, variable temperature or pressure studies are used. If appropriate, specific examples of the particular topic as applied in homogeneous hydrogenation research are detailed below.

The most popular nucleus for NMR measurements is the proton, and this is obviously related to its high sensitivity. As a rotating charged particle, a proton will generate a magnetic moment. Because, for a proton, the spin quantum number  $I=1/2$ , there are two possible spin states. In the absence of a field these states have the same energy, but in a strong magnetic field they are no longer equivalent. The population of the lower level is slightly higher than that of the upper level, according to the Boltzmann distribution. This results in a small excess magnetization vector along the z-axis. By applying a radiofrequency field for a short time, this vector can be moved and ends up in the x-y-plane ( $90^\circ$  pulse), where it will rotate. This time-response is registered by a radiofrequency coil aligned along the x-axis. This oscillatory decay (or FID) is transformed to a frequency response spectrum by the FT calculation.

## 11.2.2

**Chemical Shift**11.2.2.1 **General**

The chemical shift is caused by shielding of the proton due to a local field, generated by circulations of electrons. It is this local effect that makes it possible to use NMR as a structural characterization tool. For  $^1\text{H}$ -NMR there is a relatively straightforward correlation between chemical shift and electron density, because only diamagnetic contributions play a role, but for most other nuclei a paramagnetic term also contributes to the shielding. This makes it difficult to relate, for example, the geometry around a metal with its chemical shift [13]. For qualitative discussions of chemical shifts, the following simplified expression can be used:

$$\delta = -A + B \times (k^2 \langle r^{-3} \rangle) (\Delta E)^{-1}$$

where  $r$  is the valence shell radius and  $\Delta E$  the ligand field-splitting energy.

If either one of the terms dominates, it is sometimes possible to observe correlations. For example, a linear dependence of  $^{195}\text{Pt}$  chemical shift with UV-visible data for a series of octahedral platinum complexes has been identified [16].

Another example is the linear correlation of the  $^{59}\text{Co}$  chemical shifts of the catalyst with the regioselectivity of a trimerization reaction of acetylenes [15].

Despite the difficulties in explaining the metal NMR shifts, it is still worthwhile measuring them because the huge chemical shift range makes it easy to observe the different species present, for example diastereoisomers [18].

Bender et al. [19] used  $^{103}\text{Rh}$ -NMR chemical shift differences to demonstrate an electronic difference at rhodium between two diastereoisomers, and suggested that this might influence the crucial hydrogen addition step.

Another popular NMR nucleus is  $^{31}\text{P}$ ; this is because it is quite sensitive, it already has a large chemical shift range (as compared to  $^1\text{H}$ -NMR), the phosphorus atom is usually coupled directly to the metal atom, and phosphorus is often present in ligands of homogeneous hydrogenation complexes. Verkade [20] has reviewed aspects of  $^{31}\text{P}$ -NMR including chemical shifts, coupling constants and 2D-NMR experiments involving  $^{31}\text{P}$ .

11.2.2.2 **Chemical Shifts in Homogeneous Hydrogenation Research**

In the context of  $^1\text{H}$  chemical shifts and determination of the reaction mechanism of homogeneous hydrogenation catalysts, one usually tries to observe hydride-intermediates that typically resonate at high field (–5 to –30 ppm). Agostic bonds (see Fig. 11.1) also tend to have a hydride-like proton chemical shift.

Similarly, bridging hydrides have negative chemical shifts (e.g., at –11.18 ppm for the bridging hydride in Figure 11.2 [21]).

An excellent example of the use of  $^{31}\text{P}$  chemical shifts, in combination with  $^1\text{H}$ -NMR and  $^{103}\text{Rh}$ -NMR data as well as coupling constants information, can be found in the report by Duckett et al. [21] on the activation of

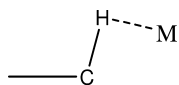


Fig. 11.1 An agostic bond.

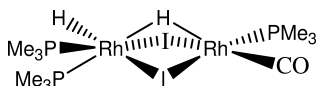
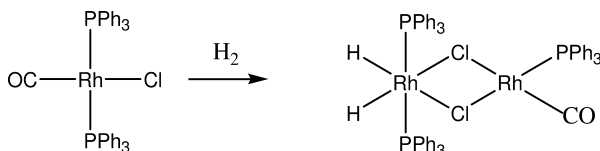


Fig. 11.2 A bridging hydride.

Fig. 11.3 Activation of  $\text{RhCl}(\text{CO})(\text{PPh}_3)_2$ .

$\text{RhX}(\text{CO})(\text{PPh}_3)_2$  [ $\text{X}=\text{halogen}$ ] complexes with hydrogen. The reaction for  $\text{X}=\text{Cl}$  is shown in Figure 11.3.

The resulting product showed a single  $^{31}\text{P}$  chemical shift at 40 ppm with a  $^1\text{J}$  coupling to rhodium of 118 Hz, indicative of a rhodium (III) center. As this rhodium atom was shown to couple to two phosphorus atoms, it could be concluded that the phosphorus atoms are in a symmetrical position, as shown in Figure 11.3. The other Rh atom couples only to a phosphorus atom with a  $^1\text{J}_{\text{RhP}}$  of 196 Hz, indicative of a rhodium (I) center.

When the smaller  $\text{P}(\text{Me})_3$  ligand was used, not only the halogens but also a hydride were found in the bridging position, as was concluded from the fact that the phosphorus atom connected to the rhodium (I) center was now coupled to a hydride.

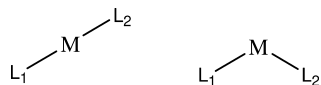
### 11.2.3

#### Coupling Constant

A second aspect that is important for the structural characterization, as mentioned above, is that of the coupling constant. Both the magnitude of the coupling constant and the multiplicity (which reflects the number of (equivalent) nuclei that couple) are important. For example, the magnitude of the  $^1\text{J}_{\text{RhH}}$  coupling constant provides information about the degree of s-character of the bond [13].

In general, in square-planar and octahedral complexes  $^1\text{J}_{\text{ML}}$  depends on the *trans*-ligand: stronger donors reduce the  $^1\text{J}_{\text{ML}}$ -value [10]. Similarly,  $^2\text{J}_{\text{L}_1\text{M,L}_2}$ -values are usually greater for *trans*-interactions than for *cis*-interactions [10], which is clearly an important tool for structural characterization (see Fig. 11.4).

The binuclear Rh-complex in Figure 11.2 contains two hydride resonances at  $-11.18$  and  $-14.75$  ppm [21]. The former has two smaller phosphorus couplings

Fig. 11.4 *Trans* (left) and *cis* (right) interactions.

( $^2J_{\text{PH}}=21$  Hz and 16 Hz) and one large coupling ( $^2J_{\text{PH}}=99.5$  Hz), indicative of a *trans* arrangement, as mentioned above. In addition, two essentially equal couplings to the two rhodium centers were found, which is consistent with the bridge position.

Gridnev et al. showed in their study of the asymmetric hydrogenation of enamides by Rh-catalysts another useful application of coupling constant patterns. By selectively labeling certain atoms, for example with  $^{13}\text{C}$  or  $^2\text{D}$ , additional couplings appear (as compared to the non-labeled product) and this will provide information about the exact structure [22].

#### 11.2.4

#### 2D-NMR

##### 11.2.4.1 General

As mentioned above, 2D-NMR (or more generally multidimensional NMR) is based on the transfer of magnetization during the evolution/mixing period.

The transfer of magnetization is not restricted to protons as in the  $^1\text{H}$ - $^1\text{H}$  COSY experiment, but can also be applied between other nuclei (i.e.,  $^1\text{H}$ - $^{13}\text{C}$ -correlation or  $^{31}\text{P}$ - $^{31}\text{P}$  correlation experiments).

A major advance in the field has been the reverse or inverse detected NMR experiment [4]. Originally, signals were enhanced by transferring magnetization from protons to insensitive nuclei that were consequently detected, as in the INEPT sequence. By reversing this process and detecting the more abundant and receptive nucleus (mostly  $^1\text{H}$ , but it can also be  $^{19}\text{F}$  or  $^{31}\text{P}$ ), the sensitivity of the experiment was greatly enhanced. An additional advantage is that the relaxation delay between the pulses is now governed by the  $^1\text{H}$  relaxation time, which is usually relatively short compared to relaxation time of other nuclei.

Technically, the inverse experiment used to be very demanding because the excess of protons not coupled to the nucleus of interest (e.g., protons coupled to the almost hundred-fold excess of  $^{12}\text{C}$  instead of  $^{13}\text{C}$ ) needed to be suppressed. Originally, this was achieved by the use of elaborate phase-cycling schemes, but today the coherence pathway selection by gradient pulses facilitates this process.

##### 11.2.4.2 2D-NMR in Homogeneous Hydrogenation Research

A variety of examples of 2D-NMR experiments is provided in reference [21]. The structure elucidation of the di-rhodium compound shown in Figure 11.3 was mostly carried out in this way. For example, 2D  $^1\text{H}$ - $^{31}\text{P}$  heteronuclear multiple quantum correlation (HMQC) experiments were used to show that two rhodium-coupled hydride resonances are connected to a single type of  $^{31}\text{P}$  nucleus.

A 2D  $^1\text{H}$ - $^{103}\text{Rh}$  HMQC experiment was used to show that both the hydrides are connected to a Rh center that resonates at 925 ppm and is coupled to two  $^{31}\text{P}$ -nuclei. A  $^1\text{H}$ - $^1\text{H}$  COSY experiment shows that the two hydrides are coupled.

An example of a  $^{103}\text{Rh}$ - $^{31}\text{P}$  correlation experiment of  $\text{Rh}(\text{MonoPhos})_2(\text{COD})\text{BF}_4$  is shown in Figure 11.5. Here also, two inequivalent  $^{31}\text{P}$  atoms are connected to the same Rh center [23].

A second class of multidimensional experiments uses through-space interactions; perhaps the best-known example is the NOESY sequence, which is as follows:

$90^\circ (+x)$  – evolution time –  $90^\circ (-x)$  – mixing time –  $90^\circ (+x)$  – acquisition

As with the COSY experiment, the sequence starts with a pulse followed by an evolution period, but now the mechanism that couples the two spins (which must be in close proximity, typically  $<6 \text{ \AA}$ ) is the Nuclear Overhauser Effect (NOE). The second pulse converts magnetization into population disturbances, and cross-relaxation is allowed during the mixing time. Finally, the third pulse transfers the spins back to the x-y-plane, where detection takes place. The spectrum will resemble a COSY spectrum, but the off-diagonal peaks now indicate through-space rather than through-bond interactions.

Just as in the COSY type of experiments this cross-relaxation effect is not restricted to protons, but can also involve heteronuclei; the acronym HOESY (heteronuclear Overhauser effect) is used in these cases. This can be used, for example, to show that an anion such as  $\text{BF}_4^-$  is in close proximity to the ligands of the organometallic compound, as was carried out by Macchioni et al. with a  $^{19}\text{F}$ - $^1\text{H}$  HOESY experiment [24].

Another important experiment here is that of EXSY (exchange spectroscopy). Here, the pulse sequence is identical to the NOESY sequence, but during the mixing time the spins physically migrate to another site due to slow chemical exchange [25]. This exchange can be both intra- and intermolecular. An example of a  $^{31}\text{P}$ - $^{31}\text{P}$  EXSY spectrum of the hydrogenation catalyst  $\text{Rh}(\text{MonoPhos})_2(\text{COD})\text{BF}_4$  is shown in Figure 11.6.

This molecule exists of isomers of the complex shown in Figure 11.7 that inter-convert rapidly, even at temperatures below 200 K, as shown by the off-diagonal peaks between the double doublets of one structure and the broad doublet of the other structure [23]. The isomeric structures are caused by the relative positions of the two ligands with respect to each other (i.e., parallel or anti-parallel orientation of the  $\text{NMe}_2$  groups).

By recording EXSY spectra at different temperatures, information can be obtained about exchange rates and activation parameters. Duckett et al. [21] used 2D-EXSY experiments to show that, for the dihydride shown in Figure 11.3, the hydride exchange process is intramolecular. The only observable off-diagonal peaks are between the two hydride resonances. Because of a negative entropy of activation of  $-61 \text{ J K}^{-1} \text{ mol}^{-1}$  it was concluded that a step with a degree of ordering is required: an additional rotation step around a Rh-halogen bond (see Fig. 11.8).



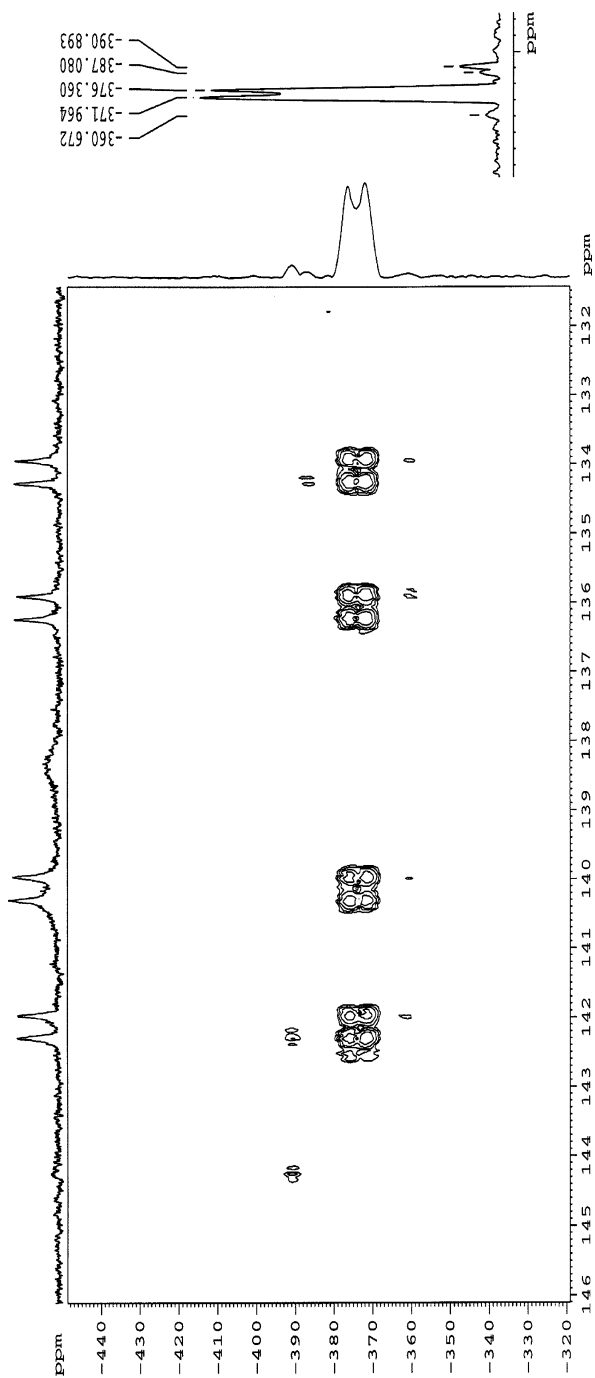


Fig. 11.5  $^{103}\text{Rh}$ - $^{31}\text{P}$  correlation experiment of  $\text{Rh}(\text{MonoPhos})_2(\text{COD})\text{BF}_4$  in  $\text{CD}_2\text{Cl}_2$  at 211 K.

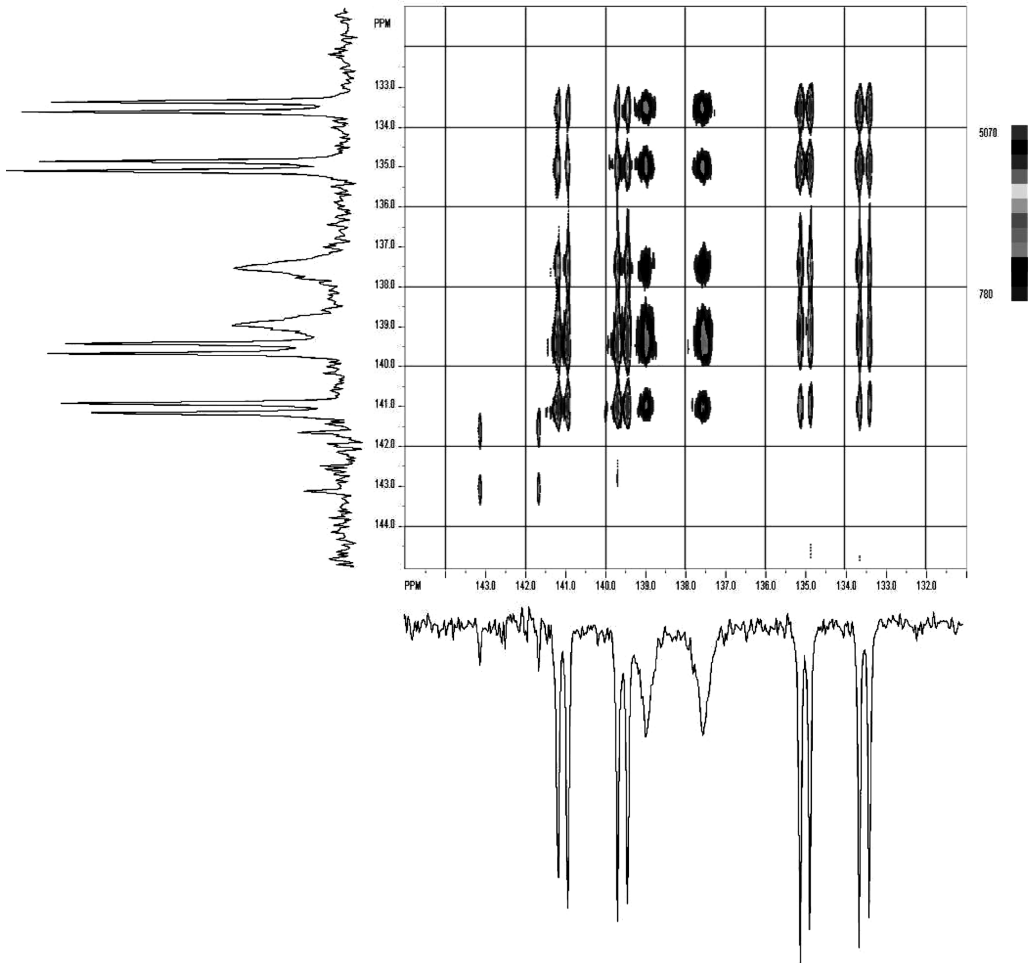


Fig. 11.6  $^{31}\text{P}$ - $^{31}\text{P}$  EXSY spectrum of  $\text{Rh}(\text{MonoPhos})_2(\text{COD})\text{BF}_4$  in  $\text{C}_2\text{D}_2\text{Cl}_2$ .

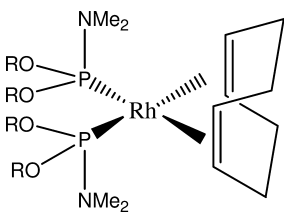


Fig. 11.7  $\text{Rh}(\text{MonoPhos})_2(\text{COD})\text{BF}_4$ .

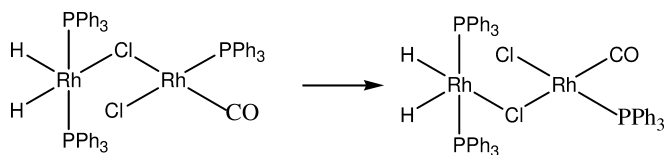


Fig. 11.8 Rotation about the Rh–Cl bond.

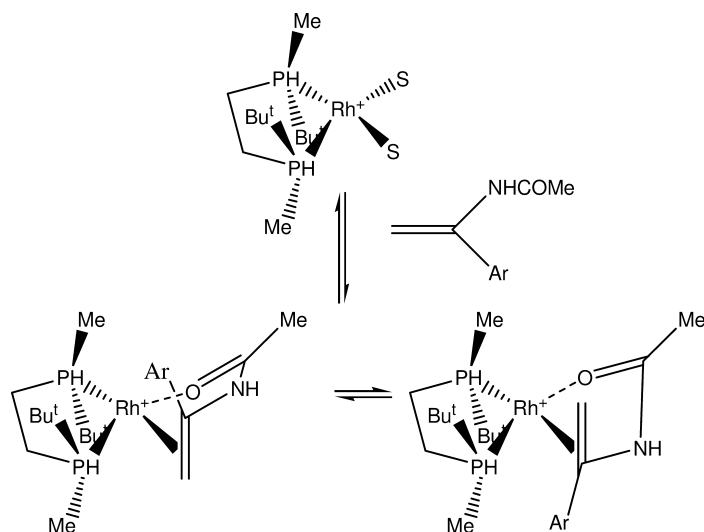


Fig. 11.9 Intermolecular exchange of Rh–*t*-Bu-BisP\* complex at 348 K.

Gridnev et al. studied the mechanism of the enantioselective hydrogenation of enamides with Rh–BisP\* and Rh–MiniPHOS catalysts [22].

By using EXSY measurements, it was shown that at 323 K there is only intramolecular exchange, whereas at 348 K intermolecular exchange also occurs via complete dissociation of the complex, producing a free substrate and a solvate complex (Fig. 11.9).

One example of the use of 2D-NMR experiments in conformational analysis is the study of molecular interactions between cinchonidine and acetic acid [26]. These alkaloids are used as chiral auxiliaries in enantioselective hydrogenations, and the enantiomeric excess is dependent on solvent polarity, acetic acid being a good solvent. This suggests that protonation and a preferred conformation play a role in achieving high enantioselectivities. With a combination of COSY-experiments,  $^3J$  coupling constants and NOESY experiments, it was shown that one conformer is preferred in acidic solutions.

## 11.2.5

## Variable Temperature and Variable Pressure Studies

## 11.2.5.1 General

Both temperature and pressure are important parameters/variables in NMR measurements of homogeneous hydrogenation catalysts. Usually, a certain hydrogen pressure is needed to form the active catalyst. The temperature controls the rate of reactions. Sometimes, temperatures above room temperature are needed; for example, the reaction shown in Figure 11.3 occurs at a hydrogen pressure of 3 atmos and temperatures above 318 K. In other cases, intermediates can only be observed at temperatures below room temperature. Modern NMR instruments routinely allow measurements to be made in the range of, for example 170 to 410 K, but this range can easily be extended by the use of special NMR probes.

As mentioned above, variable-temperature measurements are also used to obtain exchange rates and activation parameters. In the slow exchange regime, the average lifetime of a spin is long enough to observe individual lines for the various states. By increasing the exchange rate (e.g., by raising the temperature), the individual lines broaden and shift to each other until they merge into one single line. This is termed the “coalescence phenomenon” (for background information, see [27]).

## 11.2.5.2 Variable-Temperature Studies in Homogeneous Hydrogenation Research

Figure 11.10 illustrates an example of a  $^{31}\text{P}$ -NMR variable-temperature measurement, in this case of the isomeric complexes of  $\text{Rh}(\text{MonoPhos})_2(\text{COD})\text{BF}_4$  (see

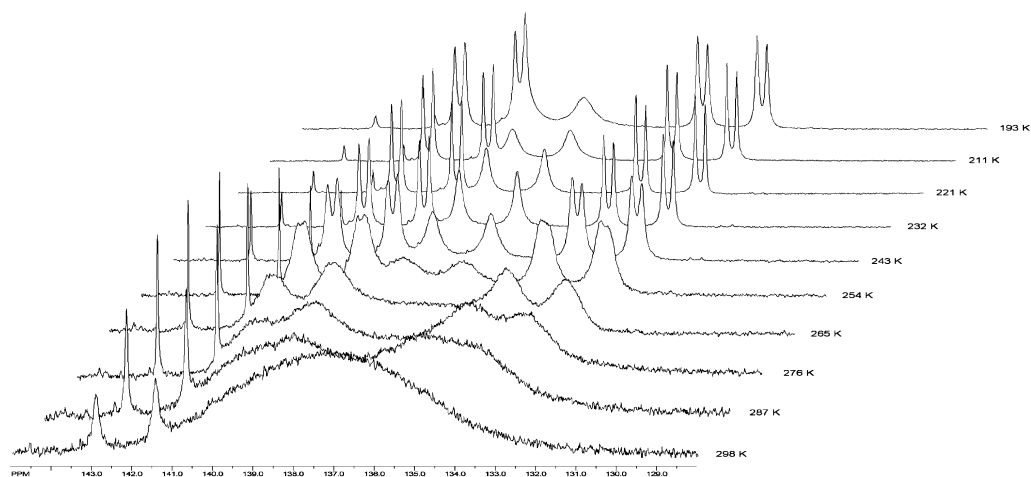


**Fig. 11.10** Temperature-dependency of  $^{31}\text{P}$ -NMR spectra of  $\text{Rh}(\text{MonoPhos})_2(\text{COD})\text{BF}_4$  in  $\text{CD}_2\text{Cl}_2$ .

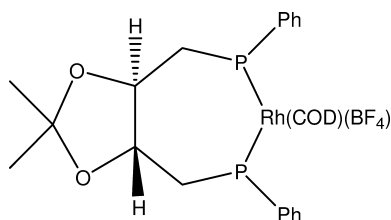


Fig. 11.11 Hydrogenation catalyst showing temperature-dependent  $^{31}\text{P}$ -NMR spectra.

Fig. 11.7) [23]. This measurement shows clearly the broadening and merging of the peaks as the temperature is increased.

Another example is the temperature-dependent study of the  $^{31}\text{P}$ -NMR spectra of the hydrogenation catalyst shown in Figure 11.11 [28]. At 240 K the  $^{31}\text{P}$ -NMR signals are equivalent, whereas at 123 K two sets of signals are observed which are attributed to a seven-membered ring in a twist-chair and a distorted boat conformation.

#### 11.2.5.3 Variable-Pressure Studies in Homogeneous Hydrogenation Research

The use of high-pressure cells and probes has been reviewed recently [29]. For homogeneous hydrogenation reactions, there is no requirement for very high pressures, and in these cases the popular sapphire tubes designed by Roe [30] will do well. In fact, the present author's group has used this type of tube in the laboratory to carry out hydrogenations, carbonylations and hydroformylations, and they have been found to be very convenient to work with. They can be pressurized in a safety hood and transported to the NMR in a transport cylinder [11]. Moreover, since the sapphire tube is transparent, color changes can also be observed.

When the tube has been placed inside the NMR spectrometer, the procedure used is exactly as for a standard NMR tube.

An example of these pressure studies is provided by the studies of Elsevier et al. [31], who investigated the dependence of the hydrogenation rate of 4-octyne by a Pd-catalyst on the dihydrogen pressure, which was varied between 0 and 40 bar. The hydrogenation rate was shown to depend linearly on the dihydrogen pressure. In order to elucidate the reaction mechanism, the dependence of the reaction rate on substrate and catalyst concentration, and on the temperature, was also measured. NMR experiments with deuterium gas as well as PHIP-experiments were also carried out.

Another interesting application of high-pressure tubes is the *in-situ* investigation of reactions in supercritical solvents such as carbon dioxide. For example, the iridium-catalyzed enantioselective hydrogenation of imines was investigated in a sapphire tube at 313 K [32].

Despite the advantages and ease of use of sapphire tubes, great care must be taken. It is very important that protective measurements are put in place when a pressurized tube is handled outside the spectrometer, because the tube's abil-

ity to cope with high pressure can be diminished if the sapphire surface is scratched. Another potentially weak point is the glue that is used to fix the titanium head to the sapphire tube. In the author's laboratory, on one occasion the head separated from the tube and was launched to the ceiling when operating close to the tube's design limits (for both temperature and pressure). Consequently, it is advised that the transport cylinder be left on top of the magnet when the tube is in the spectrometer.

#### 11.2.6

#### **PGSE NMR Diffusion Methods**

Pulsed-field gradient NMR methods are relatively new in homogeneous hydrogenation research. They allow the investigation of the diffusion of a molecule in solution by applying a defocusing and refocusing gradient pulse and measuring the decrease in intensity of the NMR signals belonging to this molecule. By carrying out a series of measurements with increasing gradient strengths, a diffusion coefficient can be calculated. If the technique is applied to a mixture of compounds and the resulting diffusion coefficients are plotted against the chemical shifts in a "2D-like fashion", the experiment is named DOSY (diffusion-ordered spectroscopy).

An example of the use of PGSE NMR spectroscopy can be found in the studies of Selke et al. [33], who investigated the dependence of enantioselectivity on the distribution of a chiral hydrogenation catalyst between aqueous and micellar phases. When a compound is incorporated into a micelle, its mobility is much lower compared to its mobility in solution. This effect is exactly what is probed with PGSE NMR. The calculated diffusion coefficient is a time-averaged value of the lower diffusion coefficient of the catalyst incorporated into the micelles, and of the diffusion coefficient of the free catalyst. An increased amount of micelle-embedded catalyst was found to lead to an increased enantioselectivity.

### 11.3

#### **Outlook**

The use of NMR continues to improve existing methods, and to develop new concepts. By cleverly combining existing pulse-sequences, new sequences are formed with improved properties. An example is the combination of the COSY and DOSY sequence to a new 3D-NMR COSY-IDOSY sequence with improved sensitivity, a 32-fold decrease in experiment time, and an improved resolution resulting in better data analysis [34].

Other developments are based on a completely new concept, for example the possibility of recording multi-dimensional NMR spectra with a single scan which, in theory, will allow the elucidation of structures to be made in seconds [35].

In time, all of these developments will be used in future chemical research studies, making NMR an even more useful tool than it is today.

## Abbreviations

DOSY	diffusion-ordered spectroscopy
EXSY	exchange spectroscopy
FT	Fourier transform
HMQC	heteronuclear multiple quantum correlation
HOESY	heteronuclear Overhauser effect
NMR	nuclear magnetic resonance
NOE	nuclear Overhauser effect
PGSE	pulsed-gradient spin echo
PHIP	<i>para</i> -hydrogen-induced polarization
ROCHESTER	Rates Of Catalytic Hydrogenation Estimated Spectroscopically Through Enhanced Resonances

## References

- 1 R. R. Ernst, W. A. Anderson, *Rev. Sci. Instr.* **1966**, *37*, 93.
- 2 J. Jeener, Ampere International Summer School, Basko Polje, Yugoslavia, **1971**.
- 3 W. P. Aue, E. Bartholdi, R. R. Ernst, *J. Chem. Phys.* **1976**, *64*, 2229.
- 4 L. Müller, *J. Am. Chem. Soc.* **1979**, *101*, 4481.
- 5 (a) R. E. Hurd, *J. Magn. Reson.* **1990**, *87*, 422; (b) A. Bax, P. G. de Jong, A. F. Mehlkopf, J. Schmidt, *Chem. Phys. Lett.* **1978**, *55*, 9.
- 6 E. O. Stejskal, J. E. Tanner, *J. Chem. Phys.* **1965**, *42*, 288.
- 7 M. Valentini, P. S. Pregosin, H. Ruegger, *Organometallics* **2000**, *19*, 2551.
- 8 W. von Philipsborn, *Chem. Soc. Rev.* **1999**, *28*, 95.
- 9 R. R. Ernst, G. Bodenhausen, A. Wokaun, *Principles of Nuclear Magnetic Resonance in One and Two Dimensions*, Oxford University Press, Oxford, **1987**.
- 10 E. M. Viviente, P. S. Pregosin, D. Scott. In: B. Heaton (Ed.), *Mechanisms in Homogeneous Catalysis. A Spectroscopic Approach*. Wiley-VCH, Weinheim, **2005**.
- 11 C. J. Elsevier, *J. Mol. Catal.* **1994**, *92*, 285.
- 12 P. S. Pregosin (Ed.), *Transition Metal Nuclear Magnetic Resonance*, Elsevier, Amsterdam, **1991**.
- 13 J. M. Ernsting, S. Gaemers, C. J. Elsevier, *Magn. Reson. Chem.* **2004**, *42*, 721.
- 14 M. S. Chinn, R. J. Eisenberg, *J. Am. Chem. Soc.* **1992**, *114*, 1908.
- 15 P. Hübler, R. Giernoth, G. Kümmerle, J. Bargon, *J. Am. Chem. Soc.* **1999**, *121*, 5311.
- 16 W. Juranic, *J. Chem. Soc., Dalton Trans.* **1984**, 1537.
- 17 W. von Philipsborn, *Pure Appl. Chem.* **1986**, *58*, 513.
- 18 C. Weidemann, W. Priebsch, D. Rehder, *Chem. Ber.* **1989**, *122*, 235.
- 19 B. R. Bender, M. Koller, D. Nanz, W. von Philipsborn, *J. Am. Chem. Soc.* **1993**, *115*, 5889.
- 20 L. D. Quin, J. G. Verkade (Eds.), *Phosphorus-31 NMR Spectral Properties in Compound Characterization and Structural Analysis*, VCH Publishers, New York, **1994**.
- 21 P. D. Morran, S. B. Duckett, P. R. Howe, J. E. McGrady, S. A. Colebrooke, R. Eisenberg, M. G. Partridge, J. A. B. Lohman, *J. Chem. Soc., Dalton Trans.* **1999**, 3949.
- 22 I. D. Gridnev, M. Yasutake, N. Higashi, T. Imamoto, *J. Am. Chem. Soc.* **2001**, *123*, 5268.
- 23 M. van den Berg, Dissertation, University of Groningen, The Netherlands, **2006**.
- 24 B. Binotti, C. Carfagna, E. Foresti, A. Macchioni, P. Sabatino, C. Zuccaccia, D. Zuccaccia, *J. Organomet. Chem.* **2004**, *689*, 647.

- 25 S. Schaeublin, A. Hoehener, R.R. Ernst, *J. Magn. Reson.* **1974**, *13*, 196.
- 26 D. Ferri, T. Bürgi, A. Baiker, *J. Chem. Soc., Perkin Trans. 2*, **1999**, 1305.
- 27 J.J. Delpuech (Ed.), *Dynamics of Solutions and Fluid Mixtures by NMR*, John Wiley & Sons Ltd, Chichester, **1995**.
- 28 R. Kadyrov, A. Borner, R. Selke, *Eur. J. Inorg. Chem.* **1999**, 705.
- 29 G. Laurency, L. Helm. In: B. Heaton (Ed.), *Mechanisms in Homogeneous Catalysis. A Spectroscopic Approach*, Wiley-VCH, Weinheim, **2005**.
- 30 D.C. Roe, *J. Magn. Reson.* **1985**, *63*, 388.
- 31 A.M. Kluwer, T.S. Koblenz, Th. Jonischkeit, K. Woelk, C.J. Elsevier, *J. Am. Chem. Soc.* **2005**, *127*, 15470.
- 32 S. Kainz, A. Brinkmann, W. Leitner, A. Pfaltz, *J. Am. Chem. Soc.* **1999**, *121*, 6421.
- 33 M. Ludwig, R. Kadyrov, H. Fiedler, K. Haage, R. Selke, *Chem. Eur. J.* **2001**, *7*(15), 3298.
- 34 M. Nilsson, A.M. Gil, I. Degadillo, G. Morris, *Chem. Commun.* **2005**, 1737.
- 35 L. Frydman, L. Lupulescu, *Proc. Natl. Acad. Sci. USA* **2002**, *99*, 15858.